Title

Metabolomic and Genomic Evidence for Compromised Bile Acid Homeostasis by Senecionine, a Hepatotoxic Pyrrolizidine Alkaloid

Journal

Chemical Research in Toxicology, 27(5)

ISSN

0893-228X

Authors

Xiong, Aizhen
Yang, Fan
Fang, Lianxiang
et al.

Publication Date

2014-05-19

DOI

10.1021/tx400451q

Peer reviewed

Published in final edited form as:

Chem Res Toxicol. 2014 May 19; 27(5): 775–786. doi:10.1021/tx400451q.

Metabolomic and Genomic Evidence for Compromised Bile Acid Homeostasis by Senecionine, a Hepatotoxic Pyrrolizidine Alkaloid

Aizhen Xiong[†,‖], **Fan Yang**[†], **Lianxiang Fang**[†], **Li Yang**[*,†], **Yuqi He**[‡], **Yvonne Yu-Jui Wan**[‡], **Ying Xu**[†], **Meng Qi**[†], **Xiuli Wang**[§], **Kate Yu**[§], **Karl Wah-Keung Tsim**[‖], **Zhengtao Wang**[*,†]

[†]The MOE Key Laboratory for Standardization of Chinese Medicines and The SATCM Key Laboratory for New Resources and Quality Evaluation of Chinese Medicines, Institute of Chinese Materia Medica, Shanghai University of Traditional Chinese Medicine, 1200 Cailun Road, Shanghai 201203, China

[‡]Department of Pathology and Laboratory Medicine, University of California, Davis, Medical Center, Room 3400B, 4645 Second Avenue, Sacramento, California 95817, United States

[§]Waters Corporation, 34 Maple Street, Milford, Massachusetts 01757, United States

[‖]Division of Life Science, Center for Chinese Medicine and State Key Laboratory of Molecular Neuroscience, The Hong Kong University of Science and Technology, Clear Water Bay Road, Hong Kong, China

Abstract

Pyrrolizidine alkaloids (PAs) are among the most hepatotoxic natural products that produce irreversible injury to humans via the consumption of herbal medicine and honey, and through tea preparation. Toxicity and death caused by PA exposure have been reported worldwide. Metabolomics and genomics provide scientific and systematic views of a living organism and have become powerful techniques for toxicology research. In this study, senecionine hepatotoxicity on rats was determined via a combination of metabolomic and genomic analyses. From the global analysis generated from two omics data, the compromised bile acid homeostasis in vivo was innovatively demonstrated and confirmed. Serum profiling of bile acids was altered with significantly elevated conjugated bile acids after senecionine exposure, which was in accordance with toxicity. Similarly, the hepatic mRNA levels of several key genes associated with bile acid metabolism were significantly changed. This process included cholesterol 7-α hydroxylase, bile acid CoA-amino acid *N*-acetyltransferase, sodium taurocholate cotransporting polypeptide, organic anion-transporting polypeptides, and multidrug-resistance-associated protein 3. In

[*]**Corresponding Authors**: (L.Y.) Phone: +86-21-51322506. Fax: +86-21-51322519. yl7@shutcm.edu.cn.; (Z.W.) Phone: +86-21-51322507. ztwang@shutcm.edu.cn.

ASSOCIATED CONTENT

Supporting Information

Quantitative ^{1}H NMR spectrum of senecionine; LC−MS chromatogram of senecionine; UPLC−MS chromatogram for metabolomic fingerprinting analysis; UPLC−MS chromatogram for bile acid profiling analysis; MS/MS fragmentation of LPC C16:0 and C18:0; primer pairs used for quantitative RT-PCR; pathways significantly interrupted after exposure to senecionine; and serum levels of bile acids. This material is available free of charge via the Internet at http://pubs.acs.org.

The authors declare no competing financial interest.

conclusion, a cross-omics study provides a comprehensive analysis method for studying the toxicity caused by senecionine, which is a hepatotoxic PA. Moreover, the change in bile acid metabolism and the respective transporters may provide a new PA toxicity mechanism.

Graphical Abstract

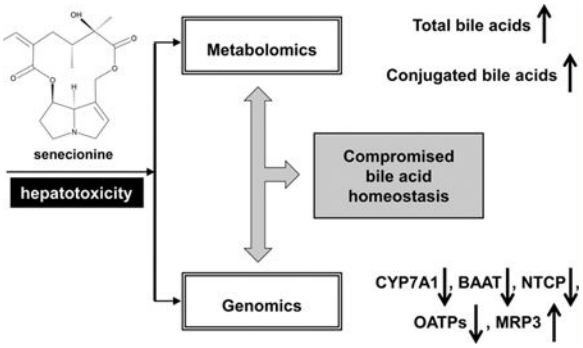

INTRODUCTION

Pyrrolizidine alkaloids (PAs) are widely distributed in over 6,000 flowering plants, especially those from the family Asteraceae, Boraginaceae, and Fabaceae, which are used to treat traumatic injury, pain, inflammation, and other ailments.[1–3] PAs are the ester derivatives of necine base and necic acid, including monoesters, noncyclic diesters, and cyclic dilactones; among these ester derivatives, cyclic dilactones with a 1,2-double bond in the necine base can induce the most potent hepatotoxicity via liver microsome activation.[3–5] Thus, these substances are called hepatotoxic pyrrolizidine alkaloids (HPAs) (Figure 1A). PAs are the most hepatotoxic natural chemicals, and they have gained global attention since the beginning of the last century. PAs produce irreversible chronic and acute hepatotoxic effects. Hepatic sinusoidal obstruction syndrome (HSOS, previously called hepatic veno-occlusive disease) is the main hepatic injury caused by PAs.[6] HSOS caused by a PA-containing herb was first reported in South Africa in 1920. Over 8,000 PA-caused poisoning cases, with estimated 2,000 deaths, have been reported in Afghanistan, China, Ethiopia, Iraq, South Africa, and Uzbekistan.[7–10] HSOS is associated with clinical symptoms, such as hepatomegaly, ascites, jaundice, and hyperbilirubinemia.[11,12] These symptoms are accompanied by 40% risk of elevated alanine aminotransferase (ALT), aspartate aminotransferase (AST), and total bilirubin (TBIL).[7,9] No effective therapies are currently available for late-stage HSOS patients. Considering the tremendous PA threat to human health, guidelines on the prevention of PA exposure have been enacted in numerous countries and organizations, such as the World Health Organization and Food and Agriculture Organization of the United Nations.[4,13–15] The International Program on Chemical Safety issued a Health and Safety Guide on PAs in 1989 and provided guidelines on exposure prevention.[15] However, toxic reports are still noted in recent years because of the intake or misuse of PA-containing herbs, such as *Gynura segetum*.[8,16] Currently, exposure to PA-containing herbs and preparations is still highly risky for human health.

In general, most PAs require metabolic activation by liver P450 enzymes, especially CYP3A isoenzymes, to form the reactive dehydrogenated pyrrolic esters.[3–5,17] These esters are unstable and act as electrophiles to covalently conjugate with nucleophiles, such as DNA, RNA, and proteins that contain thiol groups, to evoke various toxicities.[18–21] PAs induce an apoptotic DNA ladder, trigger caspase-3/−9 activation, and decrease antiapoptotic protein Bcl-xL on primary cultured mouse hepatocytes; these findings indicate that the mitochondrion-mediated apoptotic signal pathway is important for PA toxicity.[22] PAs also damage the oxidant and antioxidant balance of living organs both in vivo and in vitro.[23,24] Enhanced expressions of glutathione peroxidase 1 and glutathione *S*-transferase Pi were also found in liver tissues of mice treated with isoline, which is a cyclic diesteric PA; this finding suggested the crucial function of the liver glutathione antioxidant system for regulating PA-induced hepatotoxicity.[25] All these findings provide useful information for further study on hepatotoxic mechanisms and PA detoxification in clinics. However, the PA toxicity mechanism is still not clearly understood; thus, new technologies, such as genomics and metabolomics, may be useful for studying PA-induced hepatotoxicity.

In the past decade, omics tools have become powerful in identifying biomarkers and clarifying pathogenesis for diseases and toxicities.[26–28] These techniques are also widely used for the investigation of hepatobiliary diseases, such as nonalcoholic fatty liver disease, hepatocellular carcinoma, alcoholic liver disease, hepatitis B and C, cholestasis, and acute hepatotoxicity in animal models.[29] These studies revealed disturbed hepatic disorder of endogenous compounds, such as fatty acids,[30,31] amino acids,[32–34] and bile acids,[35–37] thereby providing new mechanisms for liver toxicity via lipogenesis, oxidative stress, phospholipid synthesis, glycolysis, cholesterol metabolism, and so on.[29]

Bile acids are the major endogenous metabolites of cholesterol. These substances are normally maintained at a balance of free and conjugated forms (as taurine conjugates and glycine conjugates) in liver and peripheral circulation. In cases of hepatobiliary and intestinal diseases, apparent changes in both the concentration of individual bile acid and the whole profile in serum, urine, and feces can be observed. Furthermore, the pattern of change varies with different pathologic features. Significantly higher serum levels of taurochenodeoxycholic acid (TCDCA), glycochenodeoxycholic acid (GCDCA), tauroursodeoxycholic acid (TUDCA), glycocholic acid (GCA), and taurocholic acid (TCA) are found in patients with severe intrahepatic cholestasis of pregnancy (ICP) than those with mild ICP, indicating that primary bile acids may be useful biomarkers for ICP clinical grading.[38] Bile acid profiling has also been studied in progressive human nonalcoholic fatty liver disease.[39] Elevated TCA and taurodeoxycholic acid (TDCA) levels are increased in liver tissues, whereas cholic acid (CA) and glycodeoxycholic acid (GDCA) levels are decreased. Meanwhile, decreased CYP 7B1 expression and increased CYP 8B1 expression are also noted in patients. All of these results suggest a transition from the classical to the alternative pathway of bile acid synthesis in the liver of patients.[39] Thus, bile acid profiling can reflect different pathologic changes and indicate the underlying pathogenesis. In addition, bile acids are also associated with PA-induced toxicity. For instance, decreased release of bile acid in PA-perfused livers and increased serum level of bile acid in PA-treated animals have been observed by researchers.[40–43] Some studies have suggested increased

serum bile acid as a sensitive index of hepatic function caused by PA.[41,42] However, this notion is not fully elucidated.

Senecionine is a 12-membered macrocyclic diester PA (Figure 1B). This alkaloid is one of the most commonly studied hepatotoxic and tumorigenic PAs. Senecionine exists in over 50 plant species, such as *Senecio vulgaris* and *Gynura segetum*, which cause several human intoxications.[4,8,16] Substantial research has revealed that senecionine-induced hepatotoxicity is associated with lipid peroxidation, intracellular Ca^{2+} alteration, and intercellular glutathione depletion.[44–46] However, these processes are not entirely responsible for cellular damage, and the mechanisms through which senecionine induces hepatotoxicity are not exclusively elucidated. In the present study, a universal metabolomics method based on liquid chromatography−mass spectrometry (LC−MS) technology and whole genome microarray was established for nontargeted study of senecionine-induced hepatotoxicity in Sprague−Dawley rats. From the cross-omics results, bile acid metabolism contributes most to the toxicity induced by senicionine. After metabolic profiling of endogenous compounds and quantitative real-time polymerase chain reaction (RT-PCR) analysis of related genes, the results revealed that compromised bile acid homeostasis is involved in senecionine-induced hepatotoxicity.

EXPERIMENTAL PROCEDURES

Chemicals and Reagents.

Senecionine was purchased from Shanghai R&D Center for Standardization of Traditional Chinese Medicine (Shanghai, China). Senecionine purity was determined to be 92% through quantitative ^1H nuclear magnetic resonance (NMR) and liquid chromatography−mass spectrometry (LC−MS) (Figures S1 and S2, Supporting Information). Bile acid standards were purchased from Sigma−Aldrich Co. (St. Louis, MO, USA), including CA, deoxycholic acid (DCA), chenodeoxycholic acid (CDCA), ursodeoxycholic acid (UDCA), hyodeoxycholic acid (HDCA), lithocholic acid (LCA), GCA, GDCA, GCDCA, glycoursodeoxycholic acid (GUDCA), glycolithocholic acid (GLCA), TCA, TDCA, taurochenodeoxycholic acid (TCDCA), TUDCA, taurohyodeoxycholic acid (THDCA), and taurolithocholic acid (TLCA). Acetonitrile and methanol were of HPLC grade and purchased from Sigma-Aldrich Co. (St. Louis, MO, USA). Ammonium acetate (99.0%, MS grade) was purchased from Sigma-Aldrich Co. (St. Louis, MO, USA). Formic acid (99.0%, HPLC grade) and ammonia solution (25.0%, HPLC grade) were purchased from Tedia Co. (Fairfield, OH, USA). Water was purified using a Millipore Milli-Q system (Billerica, MA, USA).

Animal Study and Sample Collection.

All animal studies were conducted in accordance with regulations of experimental animal administration issued by the State Committee of Science and Technology of People's Republic of China on November 14, 1988, as well as the related ethics regulations of Shanghai University of Traditional Chinese Medicine. Male Sprague−Dawley rats (n = 24, 200 to 220 g, at 6 weeks to 8 weeks of age) were used for all the experiments. Rats were housed in a strictly controlled environment for temperature and light (25 °C, 12 h light/dark

cycle), and were maintained with a commercial pellet diet and tap water ad libitum. Prior to treatment, animals were fasted overnight and divided randomly into two groups (12 rats for each group). These animals were also orally treated with sodium chloride (control group) and 35 mg/kg body weight of senecionine (treated group), respectively.

After 36 h treatment, the animals were anesthetized with ether. Blood samples were collected through the capillary vessel from the inner canthus of the eye. The blood samples were then allowed to coagulate for 2 h at room temperature. The serum samples were separated through centrifugation of the blood samples at 850*g* for 15 min at 4 °C. An aliquot of serum samples was applied for serum activity analysis of ALT, AST, and TBIL using a Hitachi automatic analyzer 7080 (Hitachi High-Tech Science Systems Corp., Ibaraki, Japan). Other serum samples were stored at −80 °C for subsequent metabolomic fingerprinting and profiling analyses. Liver samples were separated. Small blocks of left lateral lobes of the liver tissue from each rat were immediately fixed in 10% neutral formalin and embedded in paraffin for histological analysis. Five-micrometer-thick sections were stained using the hematoxylin and eosin method. Other sections were frozen in liquid nitrogen and kept at −80 °C for subsequent whole genome microarray and quantitative RT-PCR analyses.

Metabolomic Fingerprinting Analysis.

A 100 μL serum sample was diluted with an acetonitrile and methanol mixture (400 μL, v/v, 3: 1), and was centrifuged at 15,000*g* for 15 min at 4 °C to remove precipitated proteins and other particulates. All serum samples were analyzed on a Waters ACQUITY ultraperformance liquid chromatography (UPLC) system coupled with a XEVO quadruple −time-of-flight mass spectrometer (Q−TOF MS) (Waters Corp., MA, USA) in a randomized manner to minimize errors related to injection order and changes in instrument efficiency. In addition, each sample was analyzed thrice by the LC−MS system for statistical analysis.

Chromatographic conditions and mass parameters were optimized until the resolution and MS intensity of peaks did not improve observably (Figure S3, Supporting Information). Gradient chromatographic separation was performed on a Waters Aquity UPLC HSS T3 column (100 mm × 2.1 mm i.d., 1.7 μm) with a supported Security Guard HSS T3 guard column. Mobile phase A was acetonitrile, whereas mobile phase B was 5 mM ammonium acetate modified by the addition of 0.1% (v/v) formic acid. The gradient elution started with 2% mobile phase A for 1 min, which increased to 50% A at 3 min, to 60% A at 12 min, and finally to 90% A at 16 min. The mobile phase was held isocratic at 90% A for 1 min and another 3 min at 2% A before the next injection. The flow rate was 0.3 mL/min. The column was maintained at 45 °C, and the injection volume was 5 μL.

The mass spectrometer was operated in both negative and positive electrospray ionization (ESI− and ESI+) modes with MS^E technology, which can provide abundant MS/MS fragments.[47] Parameters in ESI− mode were as follows: scan range, *m*/*z* 50 to *m*/*z* 1200; capillary voltage, 2.5 kV; cone voltage, 30.0 V; source temperature, 120 °C; desolvation temperature, 350 °C; desolvation gas (nitrogen), 650.0 L/ h; cone gas (nitrogen), 30.0 L/h; and collision energy, 5 to 15 eV. Parameters in ESI+ mode were similar to those in ESI− mode, with the exception of 3.5 kV capillary voltage. A leucine−enkephalin solution (*m*/*z*

554.2615 in ESI− mode and m/z 556.2771 in ESI+ mode) was used as lock spray solvent for calculating the accurate molecular weight of biomarker candidates.

Metabolomic Profiling Analysis.

Metabolomic profiling analysis of bile acids was performed by following our previously published method.[35] In general, 100 μL of serum was diluted with 300 μL of methanol, and was centrifuged at 15,000*g* for 15 min at 4 °C to remove precipitated materials. Moreover, the supernatant was applied to a Waters ACQUITY UPLC system coupled with ZQ2000 mass spectrometer (Waters Corp., MA, USA).

Whole Genome Microarray Analysis.

The same amount of three liver samples from rats in the control group was weighed and pooled to obtain the control sample. Similarly, the same amount of three liver samples from rats in the senecionine-treated group was pooled to produce the treated sample. Total RNA was separately extracted from the two pooled samples using TRIzol Reagent (Invitrogen, Carlsbad, CA) and then prepared for labeling and hybridization to the Whole Rat Genome Oligo Microarray (4 × 44K, Agilent Technologies, covering approximately 41,000 genes). The cyanine-3-labeled RNA (cRNA) was generated from 1 μg of total RNA using the One-Color Low RNA Input Linear Amplification PLUS kit according to Agilent's Quick Amp Labeling protocol (version 5.7, Agilent Technologies). Afterward, the cyanine-3-labeled RNA (cRNA) was generated from 1 μg of pooled total RNA using the One-Color Low RNA Input Linear Amplification PLUS kit (Agilent) according to Agilent's Quick Amp Labeling protocol (version 5.7, Agilent Technologies). Dye incorporation and cRNA yield were checked using the NanoDrop ND-1000 spectrophotometer. The labeled cRNAs were then hybridized onto Agilent Whole Rat Genome Oligo Microarray according to the manufacturer's instructions. After hybridization, the slides were scanned to generate image data. Subsequently, the data were analyzed using Extraction software (Agilent, version 10.7.3.1), and genes that were differentially expressed between the control and treated groups were identified.

Analysis on mRNA Expression Level of Some Genes Associated with Bile Acid Metabolism.

Hepatic mRNA levels of some genes associated with bile acid metabolism were determined through quantitative RT-PCR. The same liver samples used for whole genome microarray analysis (i.e., three samples for each group) were extracted separately. Total RNA was extracted from liver tissue using TRIzol Reagent (Invitrogen, Carlsbad, CA) according to the manufacturer's protocol. In addition, cDNA was generated from 1 μg of RNA using a PrimeScript RT reagent kit with gDNA Eraser (Perfect Real-time) (TaKaRa, Shiga, Japan). Quantitative RT-PCR was performed using SYBR Premix Ex Taq (TaKaRa, Shiga, Japan) and ABI StepOnePlus (Applied Biosystems, Foster City, CA). Each sample was run in triplicate. Relative expression level of genes was calculated using glyceraldehyde 3-phosphate dehydrogenase (GAPDH) as the internal control. The primer pairs designed using qPrimerDepot are listed in Table S1 (Supporting Information).

Data Processing and Statistical Analysis.

The metabolomic fingerprinting spectrum was processed with MarkerLynx XS software (Waters Corp., MA, USA). The parameters were as follows: retention time (*Rt*) range, 0.5 to 16.5 min; mass range, *m*/*z* 100 to *m*/*z* 1000; and extracted ion chromatogram window (mass tolerance), 0.02 Da; width of average peak at 5% height and peak-to-peak baseline noise were automatically calculated; no smoothing was observed; marker intensity threshold: 50 counts; mass window for marker collection, 0.02 Da; retention time window for marker collection, 0.2 min; elimination level was automatically calculated; and isotopic peaks were excluded for analysis. After data processing, a list of the peak intensities was generated using *Rt* and *m*/*z* data pairs ($Rt_{m/z}$) as identifiers for each peak. The resulting 2D matrix of each peak and corresponding ion intensity (variables) for each sample (observations) were further analyzed. First, the matrix was reduced by removing any peak with missing value (ion intensity = 0) in more than 20% samples. The sets were mean-centered and pareto-scaled.[48] Afterward, the supervised orthogonal projection to latent structure-discriminant analysis (OPLS-DA) was conducted to discriminate between the samples and to determine the most important endogenous compounds related to senecionine-induced toxicity. The default seven-round cross-validation was used to guard against overfitting; 1/7th of the samples were excluded from the model in each round. Variable importance in the project (VIP) value and the OPLS-DA S-plot were used to determine potential biomarkers,[49–52] which contributed significantly to the separation between the control and the treated group. Furthermore, intensities of identified biomarkers in both control and treated groups were recorded and statistically analyzed by the two-tailed unpaired Student's *t*-test to validate the significances.

Agilent Feature Extraction software (version 10.7.3.1, Agilent Technologies) was used to analyze the acquired whole genome microarray images. Raw data containing the raw intensities of each gene detected were generated and quantile normalized using the GeneSpring GX software package (version 11.5.1, Agilent Technologies). The differentially expressed genes were then identified by setting a fold change filtering value at 2. Pathway analysis was performed in the standard enrichment computation method to determine the functions of these differentially expressed genes in the biological pathways. The enrichment *p* value of the pathway was determined using Fisher's extract test. Moreover, the false discovery rate of the pathway was also calculated. By setting the *p* value at <0.05 and the false discovery rate at <0.2,[53,54] overrepresented changed pathways were identified.

All quantitative data, including serum indexes (such as ALT activity, AST activity, and TBIL concentration), each single bile acid concentrations, and gene mRNA levels obtained via quantitative RT- PCR, were expressed as the mean ± standard error of mean (mean ± SEM) and statistically analyzed using the two-tailed unpaired Student's *t*-test. Data were considered significant (*) when $p < 0.05$ and highly significant (**) when $p < 0.01$.

RESULTS

Histopathological Examination.

The liver sections stained with hematoxylin and eosin were examined for histopathological assessment of liver injury induced by senecionine. Marked hepatocyte ballooning, diffused and hemorrhagic necrosis, blood stasis, and inflammation were clearly distinguishable in senecionine-treated rats (Figure 2B), indicating liver injury after senecionine treatment.

Assay of Biochemical Indicators.

Three common clinical biomarkers of liver injury, namely, serum ALT activity, AST activity, and TBIL concentration, were examined to evaluate the extent of senecionine-induced hepatic toxicity. At 36 h after senecionine treatment, the serum ALT activity was increased by 33-fold (1411 IU/L in treated group vs 43 IU/L in control group) (Figure 2C). Similarly, the serum AST activity was increased by 16-fold (4665 IU/L in treated group vs 286 IU/L in control group) (Figure 2D). Moreover, the serum TBIL level was elevated by 3-fold (2.4 μmol/L in treated group vs 0.8 μmol/L in control group) (Figure 2E). All of these findings suggested severe liver injury in rats treated with senecionine.

Metabolomic Fingerprinting Analysis through UPLC−QTOF−MS.

Metabolomics was performed in the present study using ESI− and ESI+ modes; in addition, the supervised OPLS-DA analytical method was introduced to distinguish the metabolomics differences between the control and the treated groups (Figure 3). Compared with the most commonly used unsupervised principle component analysis (PCA) and supervised partial least-squares−discriminant analysis (PLS-DA),[55] OPLS-DA[52,56] can improve the interpretation of resulting models, lower overfitting by rotating datum projection to maximize the separation between two classes on the X-axis, and capture unrelated or orthogonal variance on the Y-axis (such as instrumental drift and errors). Moreover, the distinct clustering of the control and treated groups can be observed in OPLS-DA models with satisfactory modeling and predictive abilities (ESI− data: $R^2Y = 0.985$, $Q^2 = 0.971$, one orthogonal and two PLS components were calculated; ESI+ data: $R2Y = 0.978$, $Q^2 = 0.961$, one orthogonal and two PLS components were calculated) (Figure 3A and B). The OPLS-DA S-plot and VIP value filter out putative biomarkers from “omics” data. By setting the VIP value at >2, 16 compounds were screened in ESI− or/and ESI+ data, which showed good covariance and correlation values in the S-plot. These compounds were further identified by comparing their retention time, accurate molecular weight, and mass fragment with those reported on web resources, such as Human Database (http://hmdb.ca), KEGG (http://www.genome.jp/kegg), and Lipidmaps (http://www.lipidmaps.org/). Among these compounds, bile acid and lysophospholipid levels were most significantly altered (Table 1). Some compounds were also authorized with available reference standards, such as CA, GCA, and TCA (Figures 3 and S2, Supporting Information).

Whole Genome Microarray of Liver Samples.

To achieve more comprehensive information after senecionine treatment, genome microarray analysis was conducted in the present study. By setting the fold change ≥2 and p

value ≤0.05, approximately 7600 genes were identified to be up-regulated or down-regulated between the control group and senecionine-treated group. The identified genes are applied to pathway analysis by setting Fisher's p value <0.05 and false discovery rate <0.2 to identify representative altered pathways, which can provide insight into the mechanisms responsive to senecionine. As a result, 46 signaling pathways were found to be down-regulated, whereas 50 signaling pathways were up-regulated after treatment (Table S2, Supporting Information). We found that genes involved in drug metabolism by cytochrome P450, peroxisome, xenobiotics metabolism by cytochrome P450, PPAR signaling pathway, bile acid excretion, fatty acid metabolism, amino acid metabolism, primary bile acid biosynthesis, and ATP-binding cassette (ABC) transporters were significantly overrepresented among down-regulated genes in the senecionine-treated group compared with the control group. These changes suggest that senecionine treatment obviously altered the biological activities of cytochrome P450- mediated metabolism, endogenous compound homeostasis, and oxidative system.

Serum Metabolomic Profiling Analysis of Bile Acids through UPLC−MS.

By combining metabolomics and microarray data, studying the alternation in the bile acid metabolism pathway after senecionine treatment has become an interesting topic. Therefore, concentrations of 17 individual bile acids, including 6 free bile acids, 5 glycine-conjugated bile acids, and 6 taurine-conjugated bile acids, were simultaneously quantified in the serum of the control and treated groups using our published method (Figure S4, Supporting Information).[35] In addition, the contents of bile acids are summarized in Figure 4 and Table S3 (Supporting Information). Compared with the control group, the concentrations of nine bile acids were significantly increased (Figure 4). Among these bile acids, TCA, TDCA, and TUDCA exhibited the highest increases of 8.1-, 6.0-, and 7.9-fold, respectively. Furthermore, four glycine-conjugated bile acids (i.e., GCA, GDCA, GUDCA, and GCDCA, and DCA) were significantly elevated in the treated group.

The total amount of free bile acids, glycine-conjugated bile acids, and taurine-conjugated bile acids were also calculated. The total amount of glycine-conjugated bile acids and taurine-conjugated bile acids in the treated group increased by 4.6-fold (4.67 μg/mL serum in the treated group vs 1.01 μg/mL serum in the control group) and 6.3-fold (3.64 μg/mL serum in the treated group vs 0.58 μg/mL serum in the treated group), respectively. The total amount of free bile acids also slightly increased by 11% (22.8 μg/mL serum in the treated group vs 20.1 μg/mL serum in the treated group).

Analysis on the mRNA Expression Level of Some Genes Associated with Bile Acid Metabolism.

On the basis of the above-mentioned results, the senecionine-induced hepatotoxicity was highly related to the bile acid metabolic network. Therefore, the relative expression of key genes involved in bile acid biosynthesis and transport pathway was further confirmed. Quantitative RT-PCR was used to validate the hepatic mRNA level of target genes, including the farnesoid X receptor (FXR); retinoic acid receptor alpha (RXRα); small heterodimer partner (SHP); cholesterol 7-alpha-hydroxylase (CYP7A1); sterol 12-α-hydroxylase (CYP8B1); bile acid-CoA amino acid *N*-acetyltransferase (BAAT); Na^+-taurocholateco-

transporting protein (NTCP); organic anion-transporting polypeptides (OATP) 2, 3, and 4; organic anion transporters (OAT) 2 and 3; bile−salt export pump (BSEP); and multidrug-resistance-associated protein (MRP) 3. As shown in Figure 5B, mRNA levels of both FXR and SHP were down-regulated after senecionine treatment. Furthermore, mRNA levels of CYP7A1, BAAT, NTCP, OATP2, and OATP4 were all down-regulated (Figure 5C). Notably, MRP3 was significantly up-regulated by more than 13-fold in the senecionine-treated group compared with the control group (Figure 5C). For other target genes, the relative expression level remained unchanged.

DISCUSSION

PAs, which are among the most toxic natural toxins, cause over 8,000 poisoning cases; this alkaloid group still threatens human health.[8–10,16] PAs are metabolized by liver cytochrome P450 enzymes, specifically CYP3A,[17] to form reactive dehydrogenated pyrrolic esters; these esters act as electrophiles and covalently conjugate with nucleophiles to evoke various toxicities.[17–21] PAs injure living organisms by triggering the mitochondria-mediated apoptotic signal pathway and damaging the balance between oxidant and antioxidant systems.[22–25] However, the pathogenesis of PA-induced hepatotoxicity is still not clear. In addition, more efforts are needed to study the hepatotoxic mechanism using powerful techniques (e.g., omics technologies), which are powerful tools for identifying biomarkers and clarifying pathogenesis for diseases and toxicities.[26–29] Therefore, metabolomic and genomic analytical methods were combined and applied in the present study.

Senecionine is one of the most commonly studied PAs; it is involved in several human intoxications.[4,8,16] Thus, senecionine was used to induce an acute toxic model on rats to study the PA-induced hepatotoxicity mechanism. PAs are toxic via metabolism by liver CYP450 enzymes; thus, a relatively higher dose is usually used to induce obvious toxicity in studying the underlying toxic mechanisms. For example, mice were treated with 100 or 110 mg/kg isoline to trigger hepatotoxicity mainly by damaging the oxidant and antioxidant balances of living organs.[23,25,44] Rats were treated with a single oral dose of 160 mg/kg of monocrotaline (equal to the estimated LD_{50} value of monocrotaline on rats by our previous study) to induce an HSOS model.[57] Large amounts of herbal extracts, for example, over 192 mg/kg alkaloid extract of *Gynura segetum* (equal to 84 mg/kg senecionine together with 60 mg/kg seneciphylline), were also used to induce severe hepatotoxicity on rats.[16] In the present study, we aimed to study acute toxicity with apparent toxic (but not lethal) injury. On the basis of our previous study, the LD_{50} in mice (i.g.) is about 57 mg/kg for senecionine,[49] which is equal to 40 mg/kg in rats. We also found that animals treated with lethal dosages died 48 h after treatment, whereas other animals that remained alive after 48 h had a great chance of surviving for more than seven days (unreported data). Therefore, 35 mg/kg of senecionine (lower than the estimated LD_{50} value) was chosen to induce significant liver injury on rats, and samples were collected 36 h after treatment when no animals died. Histological examination demonstrated that senecionine treatment resulted in clearly distinguishable liver injury. The elevated serum ALT and AST activities and TBIL levels also suggested senecionine-induced hepatocyte injury and cholestasis, which was consistent with the results of histological analysis. As reported, PAs that induce liver injury are accompanied by 40% risk of elevated ALT and AST activities and increased TBIL level.

[7,9,11,12] Thus, the hepatotoxicity induced by senecionine in the present study was regarded as a successful and typical PA-induced injury.

The liver is a vital organ that has a crucial function in metabolism and detoxification. Hepatic disorder is substantially reported to possibly disturb the balance of endogenous compounds, such as fatty acids,[30,31] amino acids,[32–35] and bile acids.[35–37,40] In the present study, some compounds of these types were also identified as potential biomarkers of senecionine-induced hepatotoxicity (Table 1). Hydroxyeicosatetraenoic acid showed the largest VIP value at ESI− mode. Hydroxyeicosatetraenoic acid is reportedly associated with liver injury caused by lipid peroxidation,[58,59] which is also responsible for PA-induced hepatotoxicity.[23–25,45] LPCs and bile acids can be detected in both ESI+ and ESI− modes. LPCs ionize much better in ESI+ mode, whereas bile acids form deprotonated ions in ESI− mode more easily. LPCs, such as LPC C18:0, C18:2, and C 18:3, have been identified as potential biomarkers for human liver cirrhosis and hepatocellular carcinoma,[46] suggesting disturbed phospholipid catabolism. Isoline-induced hepatotoxicity on mice has been reported to be connected to changes in lipid metabolism and synthesis.[25] In the current study, by comparing MS/MS fragmentations in both ESI− and ESI+ modes with known standard references LPC C16:0 and C18:0 (Figure S5, Supporting Information), several LPC C18:1, C20:4, C20:5, and C22:6, as well as their corresponding isomers, were changed in rats treated with senecionine. This finding indicates that senecionine treatment can disturb the lipid metabolism pathway. Meanwhile, three bile acids, namely, TUDCA, TCA, and GCA, were definitively identified and found to be greatly elevated after senecionine exposure.

Changes in the concentrations of these endogenous compounds were also investigated in perfused liver or plasma and bile of animals treated with herbs containing PAs.[40–43] Among these endogenous compounds, bile acids were suggested as more sensitive indices of hepatic function.[41,42] Our present study revealed changes of the total amount of bile acids and the whole profiling of individual bile acids (Figure 4 and Table S3 (Supporting Information)). Levels of taurine conjugates, glycine conjugates, and DCA were significantly increased. By contrast, CA and DCA slightly increased, whereas LCA, CDCA, and UDCA decreased (but not significantly). The results were different from those in liver injuries induced by CCl_4 and ANIT,[35–37] in which CCl_4 treatment significantly elevated CDCA, muricholic acid (MCA), UDCA, DCA, and GCA levels, whereas ANIT treatment increased GCA but decreased CDCA, MCA, UDCA, and DCA levels. CCl_4 causes free radical-induced liver injury, and ANIT results in cholestasis caused by bile duct epithelial cell injury. The difference in bile acid profiling between senecionine treatment and CCl_4 or ANIT treatment suggested a different pathogenesis for senecionine-induced toxicity, which needs further investigation.

Bile acids are normally maintained at a balance of free and conjugated forms in peripheral circulation. In cases of hepatobiliary and intestinal diseases, the balance will be damaged, especially in the synthesis, clearance, and absorption of bile acids, which are monitored by numerous transcriptional factors.[60–62] When senecionine was administered, excess bile acids accumulated in the hepatocytes and were further transported into the serum and bile driven by certain membrane transporters. Conjugated bile acids significantly increased, which indicated that the underlying mechanism was triggered to motivate synthesis, uptake, and

exportation. In the hepatocytes of liver, CA, and CDCA, two primary bile acids are catalyzed from cholesterol in the classic pathway, which further conjugate with taurine or glycine, and then reach the intestine through the bile duct to form secondary bile acids. More than 95% of the bile acids are reabsorbed and transported back to the liver via portal blood. In the entire bile acid circulation process, numerous enzymes mediate the rate-limiting steps in the biosynthesis pathway, including CYP7A1. When bile acid levels are quite high, the enzyme activity of CYP7A1 will be repressed by a nuclear receptor cascade involving FXR, which suppresses the synthesis of bile acids and maintains a balance of bile acid pool. However, as reported, FXR deficiency can lead to cholestasis conditions.[63,64] FXR−/− mice displayed significant liver injury and inflammation, and developed spontaneous liver tumors as they aged.[65] In the present study, FXR, SHP, and CYP7A1 expressions were significantly inhibited in the senecionine-treated group. Meanwhile, the histopathological features and biochemical indicators also suggested significant inflammation and cholestasis in the senecionine-treated group (Figure 2).

Approximately 95% of bile acids can be reabsorbed into hepatocytes through both sodium-dependent and -independent methods that involve NTCP and OATP. NTCP is responsible for about 75% of taurocholate uptake. Decreased NTCP and OATP expressions were found in the rat cholestasis model and patients with cholestasis liver disease.[66,67] In the current study, mRNA levels of both NTCP and OATP (i.e., OATP2 and 4) were decreased in rats treated with senecionine. These decreased reabsorption of bile acids from the portal vein was consistent with the elevated concentrations of bile acids, especially the conjugated bile acids in the serum (Figure 4 and Table S3, Supporting Information).

After being reabsorbed into hepatocytes, the bile acids are removed with high efficiency. Two patterns are involved in bile acid excretion, i.e., at the canaliculus and at basolateral membrane. BESP is the major bile acid transporter responsible for bile acid excretion into the bile canaliculus.[68,69] This transporter is highly effective in normal physiological conditions in removing bile acids. Meanwhile, protein-bound bile acids can also enter the space of Disse and are thus exposed to the basolateral membrane of the hepatocytes. Efflux of bile acids from the basolateral membrane is negligible under normal physiology. Thus, in normal circumstances, bile acid contents in the serum are low and stable. However, when cholestasis occurs, a basolateral excretion of bile acids via MRP3 is activated; MRP3 also eliminates bile acid accumulation in hepatocytes,[70,71] leading to elevated bile acid levels in the serum. After senecionine treatment, BESP expression showed no significant change. However, MRP3 expression was distinctly elevated by over 13-fold (Figure 5). Therefore, the enhanced basolateral excretion of bile acids via MRP3 increased bile acid concentration in the space of Disse, which may induce damage to sinusoidal endothelial cells and hepatocyte plasma membrane. As reported, PA-induced liver injury is highly associated with the extensive loss of sinusoidal endothelial cells and disruption of the hepatocyte plasma membrane, as well as the collagenization of the space of Disse in the later stage.[6,11,12] In the present study, an enhanced basolateral excretion of bile acids was observed in senecionine-induced hepatotoxicity, which contributed to the elevated bile acid levels in the serum (Figure 4 and Table S3, Supporting Information).

On the basis of the above discussion, compromised bile acid homeostasis was proven to have an important function in senecionine hepatotoxicity. After senecionine exposure, the detoxification process by conjugation of free bile acids to glycine and taurine via BAAT was hindered, enhancing the injury caused by the accumulation of bile salts in the hepatocytes. Meanwhile, the organism showed adaptive modulation of bile acids to prevent bile acid overload by (a) suppressing bile acid de novo synthesis via CYP7A1 inhibition; (b) limiting bile acid reabsorption by NTCP and OATP inactivation; and (c) reducing bile acid accumulation in hepatocytes via basolateral excretion by MRP3 activation, which may also result in damage to sinusoidal endothelial cells and hepatocyte plasma membrane.

CONCLUSIONS

Metabolomic and genomic technologies were first combined to study senecionine hepatotoxicity on rats, which is a new model for PA toxicological research. The results showed the reported mechanism for PA-induced toxicity (i.e., CYP450-mediated drug metabolism and apoptosis), as well as the importance of compromised bile acid homeostasis. On the basis of both changed bile acid profiling and modified bile acid transporters at transcriptional level triggered by senecionine treatment, we concluded that the bile acid metabolism pathway is strictly associated with senecionine-induced hepatotoxicity. The data presented in the current study provide important new insights into molecular and biochemical responses to senecionine-induced hepatotoxicity. Furthermore, our data provide the foundation for further evaluation on the contribution of altered bile acid metabolism in PA-induced hepatotoxicity.

Supplementary Material

Refer to Web version on PubMed Central for supplementary material.

ACKNOWLEDGMENTS

We thank KangChen Biotech (Shanghai, China) for assistance with microarray experiments.

Funding

This work was supported by the Program for Changjiang Scholars and Innovative Research Team in University (IRT1071), National Nature Science Foundation of China (81222053), Shanghai Nature Science Foundation (12ZR1450300), “Rising-Star Scholar” Project of Shanghai Municipal Science and Technology Commission (12QH1402200), Foundation for University Key Teachers of Shanghai Municipal Science and Technology (12CG50), Foundation for University Young Teachers of Shanghai Municipal Education Commission (ZZSZY12014), Hong Kong Scholars Program (XJ2012031), and China Postdoctoral Science Foundation (2012T50451).

ABRREVIATIONS

PA	pyrrolizidine alkaloid
HPA	hepatotoxic pyrrolizidine alkaloid
HSOS	hepatic sinusoidal obstruction syndrome
ALT	alanine aminotransferase

AST	aspartate aminotransferase
TBIL	total bilirubin
CA	cholic acid
MCA	muricholic acid
DCA	deoxycholic acid
CDCA	chenodeoxycholic acid
UDCA	ursodeoxycholic acid
HDCA	hyodeoxycholic acid
LCA	lithocholic acid
GCA	glycocholic acid
GDCA	glycodeoxycholic acid
GCDCA	glycochenodeoxycholic acid
GUDCA	glycoursodeoxycholic acid
GLCA	glycolithocholic acid
TCA	taurocholic acid
TDCA	taurodeoxycholic acid
TCDCA	taurochenodeoxycholic acid
TUDCA	tauroursodeoxycholic acid
HDCA	taurohyodeoxycholic acid
TLCA	taurolithocholic acid
LPS	lysophosphatide
FXR	farnesoid X receptor
SHP	small heterodimer partner
CYP7A1	cholesterol 7-α hydroxylase
CYP8B1	sterol 12-α-hydroxylase
BAAT	bile acid CoA-amino acid *N*-acetyltransferase
NTCP	sodium taurocholate cotransporting polypeptide
BSEP	bile salt export pump
MRP	multidrug-resistance-associated protein

OATP	organic anion transporting polypeptide
NMR	nuclear magnetic resonance
MS	mass spectrometry
UPLC	ultraperformance liquid chromatography
Q-TOF	quadruple-time-of-flight
VIP	variable importance in the project
OPLS-DA	orthogonal projection to latent structures−discriminant analysis
RT-PCR	real time polymerase chain reaction
LPC	lysophosphatidylcholine

REFERENCES

(1). Roeder E (1995) Medicinal plants in Europe containing pyrrolizidine alkaloids. Pharmazie 50, 83–98. [PubMed: 7700976]

(2). Roeder E (2000) Medicinal plants in China containing pyrrolizidine alkaloids. Pharmazie 55, 711–726. [PubMed: 11082830]

(3). Wiedenfeld H, and Edgar J (2011) Toxicity of pyrrolizidine alkaloids to humans and ruminants. Phytochem. Rev 10, 137–151.

(4). International Programme on Chemical Safety (1988) Pyrrolizidine Alkaloids, Environmental Health Criteria 80, WHO, Geneva, Switzerland.

(5). Fu PP, Xia QS, Lin G, and Chou MW (2004) Pyrrolizidine alkaloids-genotoxicity, metabolism enzymes, metabolic activation, and mechanisms. Drug Metabo. Rev 36, 1–55.

(6). Chojkier M (2003) Hepatic sinusoidal-obstruction syndrome: toxicity of pyrrolizidine alkaloids. J. Hepatol 39, 437–446. [PubMed: 12927933]

(7). Altaee MY, and Mahmood MH (1998) An outbreak of veno-occlusive disease of the liver in northern Iraq. East. Mediterr. Health J 4, 142–148.

(8). Dai N, Yu YC, Ren TH, Wu JG, Jiang Y, Shen LG, and Zhang J (2007) Gynura root induces hepatic veno-occlusive disease: A case report and review of the literature. World J. Gastroenterol 13, 1628–1631. [PubMed: 17461462]

(9). Kakar F, Akbarian Z, Leslie T, Mustafa ML, Watson J, Egmond HPE, Omar MF, and Mofleh J (2010) An outbreak of hepatic veno-occlusive disease in western Afghanistan associated with exposure to wheat flour contaminated with pyrrolizidine alkaloids. J. Toxicol, 1–7.

(10). Bane A, Seboxa T, Mesfin G, Ali A, Tsegaye Y, Tensae M, Selassie S, and Haile T (2012) An outbreak of veno-occlusive liver disease in northern Ethiopia, clinical findings. Ethiop. Med. J 50 (Suppl), 9–16. [PubMed: 22946291]

(11). Helmy A (2006) Review article: updates in the pathogenesis and therapy of hepatic sinusoidal obstruction syndrome. Aliment. Pharmacol. Ther 23, 11–25. [PubMed: 16393276]

(12). Wadleigh M, Ho V, Momtaz P, and Richardson P (2003) Hepatic veno-occlusive disease: pathogenesis, diagnosis and treatment. Curr. Opinion Fematol 10, 451–462.

(13). Lewis CJ (2001) Safety Alerts and Advisors: FDA Advises Dietary Supplement Manufacturers to Remove Comfrey Products from the Market, 2001, U.S. Food and Drug Administration Web site http://www.fda.gov/Food/RecallsOutbreaksEmergencies/SafetyAlertsAdvisories/ucm111219.htm (accessed Jul 6, 2001).

(14). State Pharmacopoeia Commission of the P. R. China (2010) Pharmacopoeia of the People's Republic of China, China Medicinal Science and Technology Press, Beijing, China.

(15). International Programme on Chemical Safety (1989) Pyrrolizidine Alkaloids Health and Safety Guide, Health and Safety Guide No. 26, WHO, Geneva, Switzerland.

(16). Lin G, Wang JY, Li N, Li M, Gao H, Ji Y, Zhang F, Wang HL, Zhou Y, Ye Y, Xu HX, and Zheng J (2011) Hepatic sinusoidal obstruction syndrome associated with consumption of Gynura segetum. J. Hepatol 54, 666–673. [PubMed: 21146894]

(17). Lin G, Cui YY, Liu XQ, and Wang ZT (2002) Species differences in the in vitro metabolic activation of the hepatotoxic pyrrolizidine alkaloid clivorine. Chem. Res. Toxicol 15, 1421–1428. [PubMed: 12437333]

(18). Kim HY, Stermitz FR, and Coulombe RA (1995) Pyrrolizidine alkaloid-induced DNA-protein cross-links. Carcinogenesis 16, 2691–2697. [PubMed: 7586188]

(19). Kim HY, Stermitz FR, Li JK, and Coulombe R (1999) Comparative DNA cross-linking by activated pyrrolizidine alkaloids. Food Chem. Toxicol 37, 619–625. [PubMed: 10478830]

(20). Chou MW, Jian Y, Williams LD, Xia Q, Churchwell M, Doerge DR, and Fu PP (2003) Identification of DNA adducts derived from riddelliine, a carcinogenic pyrrolizidine alkaloid, in vitro and in vivo. Chem. Res. Toxicol 16, 1130–1137. [PubMed: 12971801]

(21). Zhao Y, Xia Q, Gamboa da Costa G, Yu H, Cai L, and Fu PP (2012) Full structure assignments of pyrrolizidine alkaloid DNA adducts and mechanism of tumor initiation. Chem. Res. Toxicol 25, 1985–1996. [PubMed: 22857713]

(22). Ji LL, Chen Y, Liu TY, and Wang ZT (2008) Involvement of Bcl-xL degradation and mitochondrial-mediated apoptotic pathway in pyrrolizidine alkaloids-induced apoptosis in hepatocytes. Toxicol. Appl. Pharmacol 231, 393–400. [PubMed: 18586292]

(23). Liu TY, Wang ZY, Ji LL, and Wang ZT (2010) Pyrrolizidine alkaloid isoline induced oxidative injury in various mouse tissues. Exp. Toxicol. Pathol 62, 251–257. [PubMed: 19540740]

(24). Chen Y, Ji LL, Xiong AZ, Yang L, and Wang ZT (2013) Involvement of intracellular glutathione in regulating isoline-induced cytotoxicity in human normal liver L-02 cells. Toxicol. Ind. Health 29, 567–575. [PubMed: 22474030]

(25). Wang ZY, Kang H, Ji LL, Yang YQ, Liu TY, Cao ZW, Morahan G, and Wang ZT (2012) Proteomic characterization of the possible molecular targets of pyrrolizidine alkaloid isoline-induced hepatotoxicity. Environ. Toxicol. Pharmacol 34, 608–617. [PubMed: 22885678]

(26). Nicholson JK, Connelly J, Lindon JC, and Holmes E (2002) Metabonomics: a platform for studying drug toxicity and gene function. Nat. Rev. Drug Discovery 1, 153–161. [PubMed: 12120097]

(27). Lindon JC, Nicholson JK, Holmes E, Antti H, Bollard ME, Keun H, Beckonert O, Ebbels TM, Reily MD, Robertson D, Stevens GJ, Luke P, Breau AP, Cantor GH, Bible RH, Niederhauser U, Senn H, Schlotterbeck G, Sidelmann UG, Laursen SM, Tymiak A, Car BD, Lehman-McKeeman L, Colet JM, Loukaci A, and Thomas C (2003) Contemporary issues in toxicology the role of metabonomics in toxicology and its evaluation by the COMET project. Toxicol. Appl. Pharmacol 187, 137–146. [PubMed: 12662897]

(28). Zhang AH, Sun H, Qiu S, and Wang XJ (2013) NMR-based metabolomics coupled with pattern recognition methods in biomarker discovery and disease diagnosis. Magn. Reson. Chem 51, 549–556. [PubMed: 23828598]

(29). Beyoğlu D, and Idle JR (2013) The metabolomic window into hepatobiliary disease. J. Hepatol 59, 842–858. [PubMed: 23714158]

(30). Jiang J, Nilsson-Ehle P, and Xu N (2006) Influence of liver cancer on lipid and lipoprotein metabolism. Lipids Health Dis 5, 4–10. [PubMed: 16515689]

(31). Miyoshi H, Moriya K, Tsutsumi T, Shinzawa S, Fujie H, Shintani Y, Fujinaga H, Goto K, Todoroki T, Suzuki T, Miyamura T, Matsuura Y, Yotsuyanagi H, and Koike K (2011) Pathogenesis of lipid metabolism disorder in hepatitis C: polyunsaturated fatty acids counteract lipid alterations induced by the core protein. J. Hepatol 54, 432–438. [PubMed: 21093950]

(32). Holecek M, Mraz J, and Tilser I (1996) Plasma amino acids in four models of experimental liver injury in rats. Amino Acids 10, 229–241. [PubMed: 24178537]

(33). Wu GY (2009) Amino acids: metabolism, functions, and nutrition. Amino Acids 37, 1–17. [PubMed: 19301095]

(34). Xu Y, Yang L, Yang F, Xiong YH, and Wang ZT (2012) Metabolic profiling of fifteen amino acids in serum of chemical-induced liver injured rats by hydrophilic interaction liquid chromatograph coupled with tandem mass spectrometry. Metabolomics 8, 475–483.

(35). Yang L, Xiong AZ, He YQ, Wang ZY, Wang CH, Wang ZT, Li W, Yang L, and Hu ZB (2008) Bile acids metabonomics study on the CCl_4- and α-naphthylisothiocyanate-induced animal models: quantitative analysis of 22 bile acids by ultraperformance liquid chromatography- mass spectrometry. Chem. Res. Toxicol 21, 2280–2288. [PubMed: 19053324]

(36). Wang R, Xiong AZ, Teng ZQ, Yang QW, Shi YH, and Yang L (2012) Radix Paeoniae Rubra and Radix Paeoniae Alba attenuate CCl4-induced acute liver injury: An ultra-performance liquid chromatography-mass spectrometry (UPLC-MS) based metabolomic spproach for the pharmacodynamic study of traditional Chinese medicines (TCMs). Int. J. Mol. Sci 13, 14634–14647. [PubMed: 23203085]

(37). Yang F, Xu Y, Xiong AZ, He YQ, Yang L, Wan Y-JY, and Wang ZT (2012) Evaluation of the protective effect of Rhei Radix et Rhizoma against α-naphthylisothiocyanate induced liver injury based on metabolic profile of bile acids. J. Ethnopharmacol 144, 599–604. [PubMed: 23058990]

(38). Chen J, Deng W, Wang J, Shao Y, Ou M, and Ding M (2013) Primary bile acids as potential biomarkers for the clinical grading of intrahepatic cholestasis of pregnancy. Int. J. Gynaecol. Obstet 1, 5–8.

(39). Lake AD, Novak P, Shipkova P, Aranibar N, Robertson D, Reily MD, Lu Z, Lehman-McKeeman LD, and Cherrington NJ (2013) Decreased hepatotoxic bile acid composition and altered synthesis in progressive human nonalcoholic fatty liver disease. Toxicol. Appl. Pharmacol 2, 132–140.

(40). Lessard P, Wilson WD, Olander HJ, Rogers QR, and Mendel VE (1986) Clinicopathologic study of horses surviving pyrrolizidine alkaloid (Senecio vulgaris) toxicosis. Am. J. Vet. Res 47, 1776–1780. [PubMed: 2875683]

(41). Mendel VE, Witt MR, Gitchell BS, Gribble DN, Rogers QR, Segall HJ, and Knight HD (1988) Pyrrolizidine alkaloid-induced liver disease in horses: an early diagnosis. Am. J. Vet. Res 49, 572–578. [PubMed: 3377320]

(42). Sutherland RJ, Deol HS, and Hood PJ (1992) Changes in plasma bile acids, plasma amino acids, and hepatic enzyme pools as indices of functional impairment in liver-damaged sheep. Vet. Clin. Pathol 21, 51–56. [PubMed: 12671802]

(43). Yan CC, and Huxtable RJ (1995) Relationship between glutathione concentration and metabolism of the pyrrolizidine alkaloid, monocrotaline, in the isolated, perfused liver. Toxicol. Appl. Pharmacol 130, 132–139. [PubMed: 7839360]

(44). Liang QN, Sheng Y, Jiang P, Ji LL, Xia Y, Min Y, and Wang ZT (2011) The gender-dependent difference of liver GSH antioxidant system in mice and its influence on isoline-induced liver injury. Toxicology 280, 61–69. [PubMed: 21126554]

(45). Griffin DS, and Segall HJ (1987) Lipid peroxidation and cellular damage caused by the pyrrolizidine alkaloid senecionine, the alkenal trans-4-hydroxy-2-hexenal, and related alkenals. Cell Biol. Toxicol 3, 379–390. [PubMed: 3507264]

(46). Griffin DS, and Segall HJ (1987) Role of cellular calcium homeostasis in toxic liver injury induced by the pyrrolizidine alkaloid senecionine and the alkenal trans-4-OH- 2-hexenal. J. Biochem. Toxicol 2, 155–167. [PubMed: 3508471]

(47). Castro-Perez JM, Kamphorst J, DeGroot J, Lafeber F, Goshawk J, Yu K, Shockcor JP, Vreeken RJ, and Hankemeier T (2010) Comprehensive LC-MSE lipidomic analysis using a shotgun approach and its application to biomarker detection and identification in osteoarthritis patients. J. Proteome. Res 9, 2377–2389. [PubMed: 20355720]

(48). Van den Berg RA, Hoefsloot HC, Westerhuis JA, Smilde AK, and van der Werf MJ (2006) Centering, scaling, and transformations: improving the biological information content of metabolomics data. BMC Genomics 7, 142–156. [PubMed: 16762068]

(49). Xiong AZ, Yang L, Ji LL, Wang ZY, Yang XJ, Chen Y, Wang XL, Wang CH, and Wang ZT (2012) UPLC-MS based metabolomics study on two Senecio herbs, Senecio scandens and S. vulgaris: an approach for the differentiation of genetically closed species with similar morphology but different toxicity. Metabolomics 8, 614–623.

(50). Wiklund S, Johansson E, Sjostrom L, Mellerowicz EJ, Edlund U, Shockcor JP, Gottfries J, Moritz T, and Trygg J (2008) Visualization of GC/TOF-MS-based metabolomics data for identification of biochemically interesting compounds using OPLS class models. Anal. Chem 80, 115–122. [PubMed: 18027910]

(51). Xie GX, Ni Y, Su MM, Zhang YY, Zhao AH, Gao XF, Liu Z, Xiao PG, and Jia W (2008) Application of ultraperformance LC-TOF MS metabolite profiling techniques to the analysis of medicinal Panax herbs. Metabolomics 4, 248–260.

(52). Yin PY, Wan DF, Zhao CZ, Chen J, Zhao XJ, Wang WZ, Lu X, Yang SL, Gu JR, and Xu GW (2009) A metabonomic study of hepatitis B-induced liver cirrhosis and hepatocellular carcinoma by using RP-LC and HILIC coupled with mass spectrometry. Mol. Biosyst 5, 868–876. [PubMed: 19603122]

(53). Bittel DC, Kibiryeva N, and Butler MG (2007) Whole genome microarray analysis of gene expression in subjects with fragile X syndrome. Genet. Med 9, 464–472. [PubMed: 17666893]

(54). Li Y, Wang H, Yang B, Yang J, Ruan X, Yang Y, Wakeland EK, Li Q, and Fang X (2012) Influence of carbon monoxide on growth and apoptosis of human umbilical artery smooth muscle cells and vein endothelial cells. Int. J. Biol. Sci 8, 1431–1446. [PubMed: 23197940]

(55). Boulesteix AL, and Strimmer K (2006) Partial least squares: A versatile tool for the analysis of high dimensional genomic data. Briefing Bioinf 8, 32–44.

(56). Trygg J, and Wold S (2002) Orthogonal projections to latent structures (O-PLS). J. Chemom 16, 119–128.

(57). DeLeve LD, McCuskey RS, Wang X, Hu L, McCuskey MK, Epstein RB, and Kanel GC (1999) Characterization of a reproducible rat model of hepatic veno-occlusive disease. Hepatology 29, 1779–1791. [PubMed: 10347121]

(58). Morita M, Ishida N, Uchiyama K, Yamaguchi K, Itoh Y, Shichiri M, Yoshida Y, Hagihara Y, Naito Y, Yoshikawa T, and Niki E (2012) Fatty liver induced by free radicals and lipid peroxidation. Free Radical Res 46, 758–765. [PubMed: 22468959]

(59). Niki E (2014) Biomarkers of lipid peroxidation in clinical material. Biochim. Biophys. Acta 1840, 809–817. [PubMed: 23541987]

(60). Claudel R, Steals B, and Kuipers F (2005) The farnesoid X receptor: A molecular link between bile acid and lipid and glucose metabolism. Arterioscler., Thromb., Vasc. Biol 25, 2020–2030. [PubMed: 16037564]

(61). Calkin AC, and Tontonoz P (2012) Transcriptional integration of metabolism by the nuclear sterolactivated receptors LXR and FXR. Nat. Rev. Mol. Cell Biol 13, 213–224. [PubMed: 22414897]

(62). Nicolaou M, Andress EJ, Zolnerciks JK, Dixon PH, Williamson C, and Linton KJ (2012) Canalicular ABC transporters and liver disease. J. Pathol 226, 300–315. [PubMed: 21984474]

(63). Wu XP, Chai J, and Chen WS (2009) Changes of cholesterol 7alpha-hydroxylase, farnesoid X receptor, and heterodimer partner expression in liver tissues of rats with obstructive cholestasis. Acad. J. Sec. Mil. Med. Univ 30, 1398–1401.

(64). Abu-Hayyeh S, Papacleovoulou G, Lovgren-Sandblom A, Tahir M, Oduwole O, Jamaludin NA, Ravat S, Nikolova V, Chambers J, Selden C, Rees M, Marschall HU, Parker MG, and Williamson C (2013) Intrahepatic cholestasis of pregnancy levels of sulfated progesterone metabolites inhibit FXR resulting in a pro-cholestatic phenotype. Hepatology 57, 716–726. [PubMed: 22961653]

(65). Yang F, Huang XF, Yi TS, Yen Y, Moore DD, and Huang WD (2007) Spontaneous development of liver tumors in the absence of the bile acid receptor farnesoid X receptor. Cancer Res 67, 863–867. [PubMed: 17283114]

(66). Zollner G, Fickert P, Zenz R, Fuchsbichler A, Stumptner C, Kenner L, Ferenci P, Stauber RE, Krejs GJ, Denk H, Zatloukal K, and Trauner M (2004) Hepatobiliary transporter expression in percutaneous liver biopsies of patients with cholestatic liver diseases. Hepatology 33, 633–646.

(67). Geier A, Dietrich CG, Gerloff T, Haendly J, Kullak-Ublick GA, Stieger B, Meier PJ, Matern S, and Gartung C (2003) Regulation of basolateral organic anion transporters in ethinylestradiol-induced cholestasis in the rat. Biochim. Biophys. Acta 1609, 87–94. [PubMed: 12507762]

(68). Stieger B, Fattinger K, Madon J, Kullak-Ublick GA, and Meier PJ (2000) Drug- and estrogen-induced cholestasis through inhibition of the hepatocellular bile salt export pump (Bsep) of rat liver. Gastroenterology 118, 422–430. [PubMed: 10648470]

(69). Cao J, Huang L, Liu Y, Hoffman T, Stieger B, Meier PJ, and Vore M (2001) Rregulation of hepatic bile salt and organic anion transporters in pregnant and postpartum rats and the role of prolactin. Hepatology 33, 140–147. [PubMed: 11124830]

(70). Soroka CJ, Lee JM, Azzaroli F, and Boyer JL (2001) Cellular localization and up-regulation of multidrug resistance-associated protein 3 in hepatocytes and cholangiocytes during obstructive cholestasis in rat liver. Hepatology 33, 783–791. [PubMed: 11283840]

(71). Teng S, and Piquette-Miller M (2007) Hepatoprotective role of PXR activation and MRP3 in cholic acid-induced cholestasis. Br. J. Pharmacol 151, 367–376. [PubMed: 17435798]

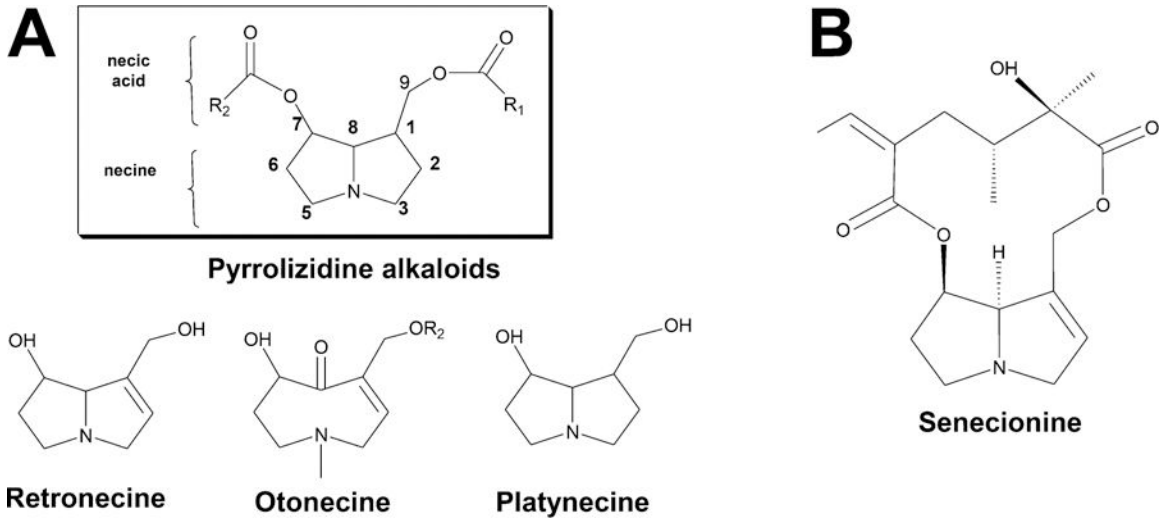

Figure 1.
Pyrrolizidine alkaloid structures. (A) Common structures of pyrrolizidine alkaloids. (B) The structure of senecionine.

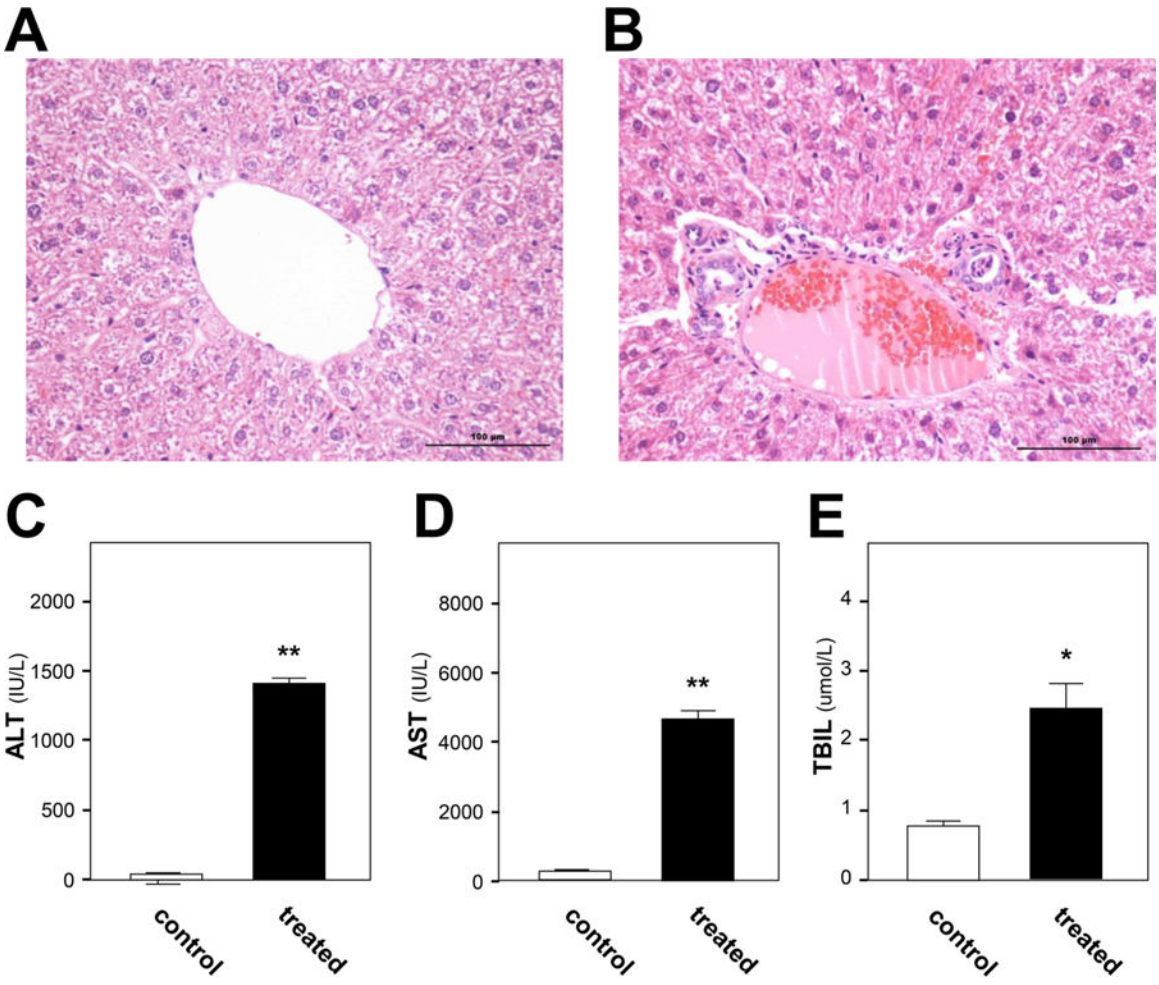

Figure 2.

Histological and biochemical findings of toxicity caused by senecionine in rats. A and B show liver sections of rats from the control group and senecionine-treated group, respectively. The bar represents 100 μm. C, D, and E show serum ALT activity, AST activity, and TBIL level, respectively. Values are expressed as the mean ± SEM; significant differences between the control group ($n = 12$) and treated group ($n = 12$) are based on two-tailed unpaired Student's t-tests (*$p < 0.05$ and **$p < 0.01$).

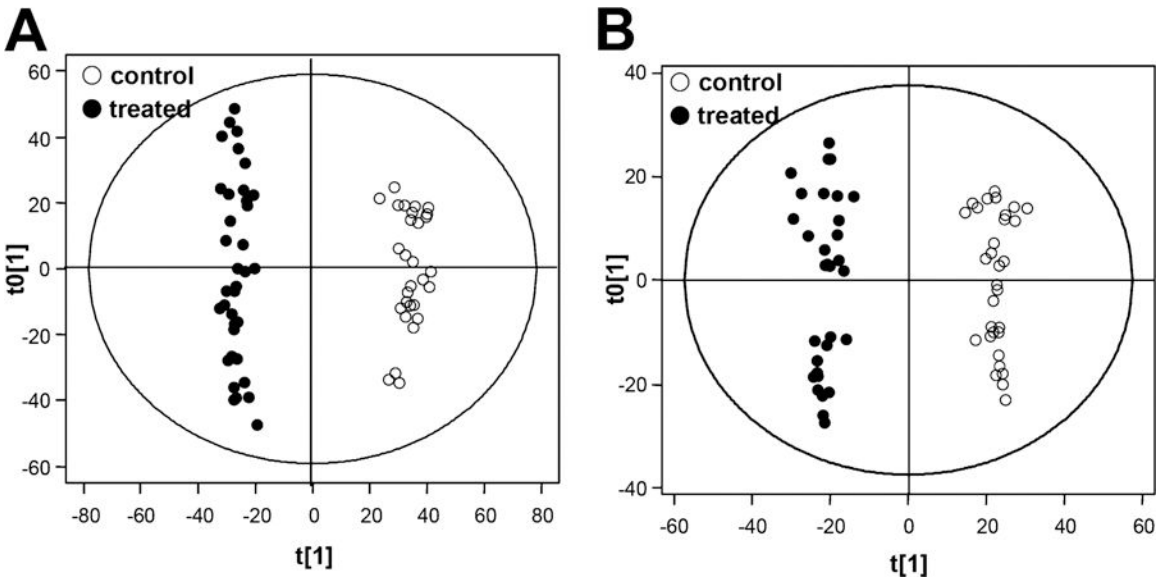

Figure 3.

Results of OPLS-DA analysis of the control and senecionine-treated groups. A shows the OPLS-DA score plots generated by ESI- data; B shows the OPLS-DA score plots generated by ESI+ data. (○) represents the control group; and (●) represents the senecionine-treated group. All data were generated through UPLC−QTOF−MS analysis.

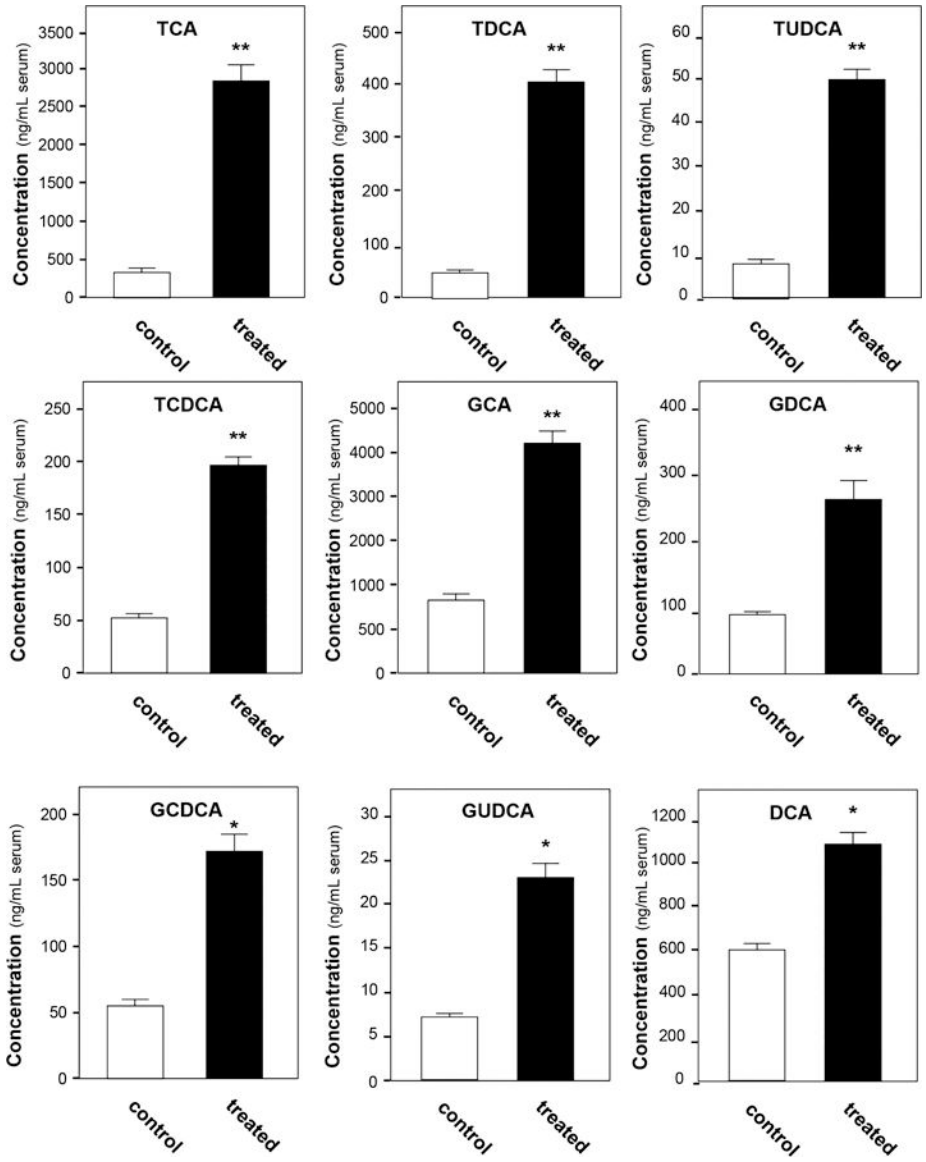

Figure 4.

Serum bile acid content significantly changed in the senecionine-treated group. Values were expressed as the mean ± SEM; significant differences between the control group ($n = 12$) and treated group ($n = 12$) are based on two-tailed unpaired Student's *t*-tests (*$p < 0.05$ and **$p < 0.01$). All data were generated through UPLC−MS analysis.

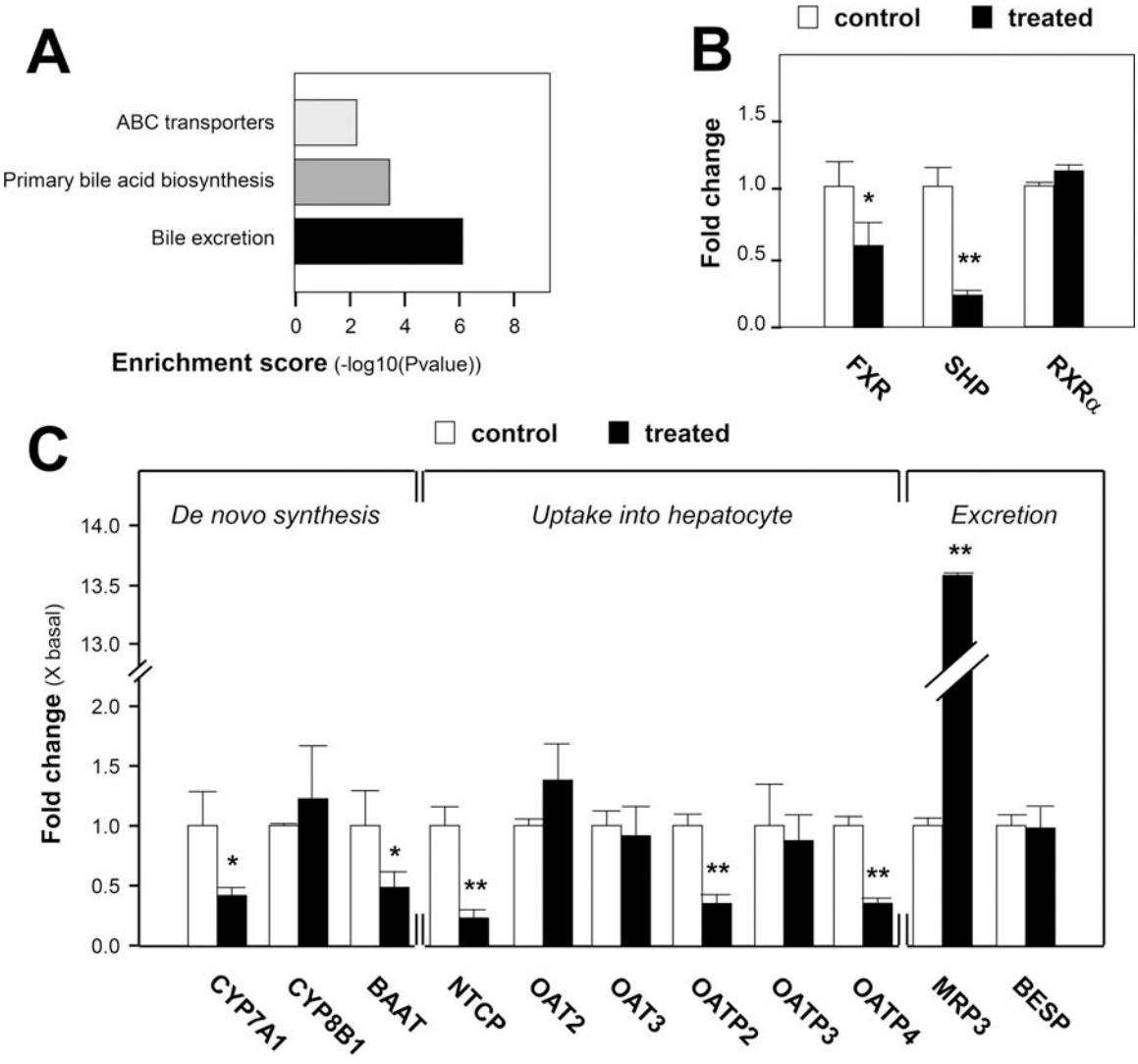

Figure 5.

Genome evidence for altered bile acid homeostasis after exposure to senecionine. A shows some significantly changed pathways. Data were generated by whole genome microarrays. Enrichment Score stands for the enrichment score value of the pathway, which is equal to −log10(*P* value). B and C show the relative expression of some genes associated with bile acid metabolism in the senecionine-treated group compared with those in the control group. Hepatic mRNA levels were determined through quantitative RT-PCR, with GAPDH as the internal standard. Relative gene expression was calculated as the ratio of mRNA level in the treated group to that in the control group; this value is expressed as the mean ± SEM; significant differences between the control group ($n = 3$) and treated group ($n = 3$) are based on two-tailed unpaired Student's *t*-tests (*$p < 0.05$ and **$p < 0.01$).

Table 1.

Potential Endogenous Biomarkers[a]

t_R (min)	*m/z*	mass accuracy(ppm)	metabolite	fold change compared with controls
3.61	512.2651[b]	5.77	sulfolithocholylglycine	13.1 ↑
3.79	498.2854[b]	6.93	tauroursodeoxycholic	11.0 ↑
3.82	514.2803[b]	6.66	taurocholic acid[d]	11.3 ↑
4.08	455.2476[b]	2.17	sulfolithocholic acid	20.5 ↑
4.26	464.298[b]	6.64	glycocholic acid[d]	4.3 ↑
4.66	407.277[b]	6.44	β-muricholic acid	1.6 ↓
5.41	542.3245[c]	0.50	LPC C20:5	3.6 ↓
8.86	544.3402[c]	0.40	LPC C20:4 isomer	1.5 ↓
9.33	544.3404[c]	0.04	LPC C20:4	1.5 ↓
9.41	568.3410[c]	1.02	LPC C22:6	66.3 ↑
10.87	522.3545[c]	3.01	LPC C18:1 isomer	2.1 ↓
11.07	522.3553[c]	1.48	LPC C18:1 isomer	2.2 ↑
11.81	522.3559[c]	0.33	LPC C18:1	3.4 ↑
12.73	319.2277[b]	1.56	hydroxyeicosatetraenoic acid	2.5 ↓
16.13	301.2153[b]	4.43	eicosapentaenoic acid	1.9 ↑
16.22	277.2145[b]	7.69	linolenic acid	1.8 ↑

[a] Many biomarkers can be detected in both ESI+ and ESI− modes.

↑ means up-regulated in the treated group compared with the control group, while ↓ means down-regulated in the treated group compared with the control group.

[b] Data of compounds are from those detected in ESI- mode while.

[c] Data were from those in ESI+ mode.

[d] Markers confirmed by standard compounds.